



# Geophysical Research Letters

## RESEARCH LETTER

10.1029/2018GL077734

**Key Points:**

- Western disturbances (WDs) and Tibetan Plateau vortices (TPVs) are tracked in ERA-Interim reanalysis
- WD and TPV frequencies are anticorrelated during the annual cycle, controlled by jet latitude
- Interannual variability of WD and TPV occurrence is strongly controlled by upper-level baroclinicity

**Correspondence to:**

K. M. R. Hunt,  
k.m.r.hunt@reading.ac.uk

**Citation:**

Hunt, K. M. R., Curio, J., Turner, A. G., & Schiemann, R. (2018). Subtropical westerly jet influence on occurrence of western disturbances and Tibetan Plateau vortices. *Geophysical Research Letters*, 45, 8629–8636.  
<https://doi.org/10.1029/2018GL077734>

Received 1 MAR 2018

Accepted 5 AUG 2018

Accepted article online 13 AUG 2018

Published online 23 AUG 2018

## Subtropical Westerly Jet Influence on Occurrence of Western Disturbances and Tibetan Plateau Vortices

**K. M. R. Hunt<sup>1</sup> , J. Curio<sup>1,2</sup> , A. G. Turner<sup>1,2</sup>, and R. Schiemann<sup>1,2</sup>**

<sup>1</sup>Department of Meteorology, University of Reading, Reading, UK, <sup>2</sup>National Centre for Atmospheric Science, University of Reading, Reading, UK

**Abstract** Western disturbances (WDs) are midtropospheric to upper-tropospheric mesoscale vortices, which typically propagate along the subtropical westerly jet stream and bring heavy rainfall to Pakistan and northern India during boreal winter. They are dynamically similar to Tibetan Plateau vortices (TPVs), which affect southwest China during spring and summer and emanate from the Tibetan Plateau. Here we propose that their similarity implies the existence of a more general group of upper-tropospheric vortices featuring interactions with the orography of the Hindu Kush-Himalaya-Tibetan Plateau region. Using existing track databases for WDs and TPVs derived from ERA-Interim reanalysis, we show that their respective occurrence frequencies are highly anticorrelated with each other through the seasonal cycle, yet both are strongly correlated with jet latitude. Our findings imply that the incidence of hazards due to WDs and TPVs is correlated on intra-annual and interannual time scales, particularly through upper-level baroclinicity.

**Plain Language Summary** North India and south China (including Tibet) experience seasonal midlevel cyclonic systems, referred to as western disturbances (WDs) and Tibetan Plateau vortices (TPVs), respectively. These systems can be responsible for heavy, even catastrophic, rainfall in the areas associated with them, and thus improving prediction and risk correlation is vital. In this study, we show that: first, previous literature alludes to the two types of system bearing similar structures; second, the mean annual cycles of both are strongly affected by the subtropical westerly jet; third, the interannual populations of each are related; and fourth, this relationship can be explained by considering features of the jet, such as strength and position. We thus conclude that it is likely that WDs and TPVs are specific examples of a more general class of synoptic-scale vortex.

### 1. Introduction

The climates of Pakistan, northern India, and southwest China encompassing the Tibetan Plateau are strongly influenced by seasonal midtropospheric synoptic-mesoscale vortices. Over Pakistan/northern India, where these mesoscale vortices interact with the Hindu Kush and Karakoram mountain ranges, they are called western disturbances (WDs; Pisharoty & Desai, 1956); over southwest China, where they interact with the Tibetan Plateau, they are called Tibetan Plateau vortices (TPVs; Tao & Ding, 1981). Formally, a TPV is defined as “a shallow meso- $\alpha$ -scale cyclonic vortex that is usually confined to near-surface levels (500 hPa) over the Tibetan Plateau during warm seasons” (Feng et al., 2014); and a WD as a: “cyclonic circulation in the midtropospheric and lower-tropospheric levels or as a low pressure area on the surface, which occurs in middle latitude westerlies and originates over the Mediterranean Sea, Caspian Sea and Black Sea and moves eastward across north India” (<http://imd.gov.in/section/nhac/wxfaq.pdf>).

There is an additional class of mesoscale vortex that brings rain to this region, the southwest vortex (SWV), which typically spins up to the east of the Tibetan Plateau (Li et al., 2017). However, they are physically distinct from both TPVs and WDs whose vorticity maxima are at 450 (Feng et al., 2017; Zheng et al., 2013) and 350 hPa (Hunt et al., 2017), respectively, in having a vorticity maximum at 750 hPa (Feng et al., 2016); furthermore, the vertical extents are different, for example, an average WD has a significant positive vorticity anomaly between 600 and 200 hPa, whereas SWVs typically extend from the surface to 500 hPa. While they can interact constructively with TPVs to produce heavy rain (Chen et al., 1996; Li et al., 2017), they are generally considered to be structurally unrelated (Feng et al., 2014; 2016) and are not considered here.

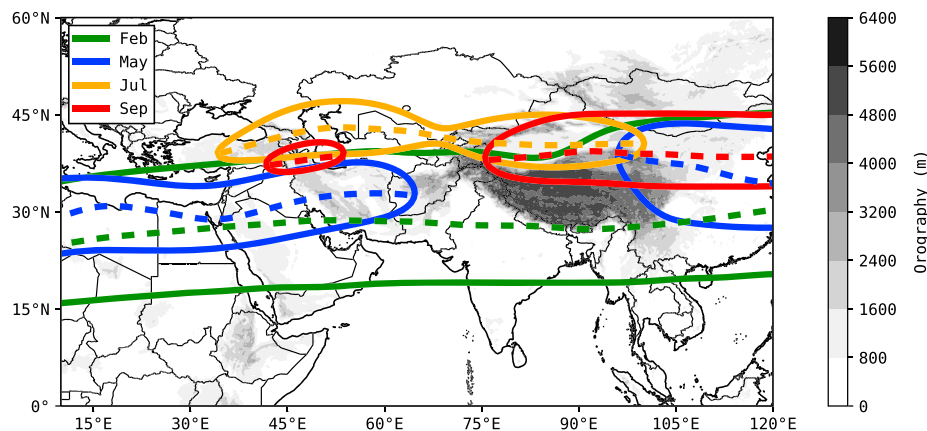


**Figure 1.** Mean 200 hPa isotachs for 80th percentile zonal wind in selected months: winter (February, green, 25.0 m/s), pre-monsoon (May, blue, 24.5 m/s), monsoon (July, yellow, 22.9 m/s), and post-monsoon (September, red, 24.6 m/s). Dashed lines indicate the mean axis of the jet for that month. Orography contours are also given.

WDs and TPVs are important since they can be responsible for storms and heavy rainfall both through convergence-driven and orographic ascent, in areas where seasonal rainfall is otherwise not particularly high (Hunt et al., 2018; Li et al., 2017). If there was a relationship between these two types of system, it would have important consequences in understanding correlated risks of extreme weather in the region.

The structure of WDs has been explored in detail in both case studies (e.g., Dimri, 2004; Ramanathan & Saha, 1972) and composite studies (Hunt et al., 2017); and while the quantity of analogous research on TPVs is markedly less in the English literature, there have been several case studies (Dell'Osso & Chen, 1986; Wang, 1987) as well as a composite study (Feng et al., 2017). These studies indicate that despite substantial interpopulation variance, there are strong similarities between TPVs and WDs, for example, a warm-over-cold thermal structure, a quadrupolar signature in divergence, and a tropospheric vorticity column indicative of baroclinic growth. There are some differences too though, in how they organize local humidity, which differs in the large scale between the plateau and the Indian subcontinent, and vorticity, which is influenced by sensible heating from the plateau in the case of TPVs. Furthermore, both have similar annual frequencies and climatologically move eastward at similar speeds (Feng et al., 2014; Hunt et al., 2017). These studies, among others (e.g., Li et al., 2011), further highlight the importance of the jet, in the northern half of which such vortices are often embedded.

It is also important to note that proposed genesis mechanisms for WDs and TPVs differ. WDs are thought to originate as extratropical cyclones or perturbations in the jet that are subsequently intensified by downstream barotropic or baroclinic instability (Hunt et al., 2017; Mull & Desai, 1947). In contrast, the origin of TPVs is thought to be diabatic heating of the Tibetan Plateau (Li, Zhang, & Wen, 2014; Li, Zhang, Wen, & Liu, 2014) with a smaller dynamic contribution (Zheng et al., 2013). That is not to say that the jet might not be somehow coupled with the surface heating (Kuang & Zhang, 2005).

Figure 1 shows the climatology of the jet for selected months from 1979 to 2017 using ERA-Interim data. For each month, the solid lines show the locations of isotachs representing the 80th percentile zonal wind speed at 200 hPa (for a given month), which is typically around 25 m/s. For these regions of high wind speed, dashed lines indicate the meridional maximum—the so-called jet axis. During boreal winter (green), the jet is strongest and furthest south, with the axis typically lying over northern India. As the Indian summer monsoon starts to develop (May; in blue), warming of the Tibetan Plateau establishes tropospheric temperature gradients both to the north and south. While the tropical easterly jet is established on its southern side (not shown), over India, the subtropical westerly jet is pushed to the north and weakened, a situation that reaches its apex during July (yellow), where the jet completely avoids India, before beginning to return to the winter pattern as the monsoon retreats (red).

It is therefore evident that both the strength and latitude of the jet have a strong dependence on season. Given the dependence of TPV and WD populations on jet position, we pose two hypotheses: first, we expect a phased relationship between their mean seasonal cycles of occurrence; second, we expect some interannual

correlation in their occurrence, especially in months where variability in jet latitude is high (Schiemann et al., 2009) and where both populations are significant. While there have been a few studies on the dynamics of both WDs and TPVs (e.g., Li et al., 2002; Li & Liu, 2006; Raju et al., 2011), no attempt has been made to explore the relationship between them.

## 2. Data and Methods

### 2.1. Track Databases

#### 2.1.1. Western Disturbances

We use the WD database produced by Hunt et al. (2017). They used T5-T63 spectrally band-passed midtropospheric (450–300 hPa) relative vorticity to identify 3,090 WD tracks in ERA-Interim from 1979 to 2016. They include a domain-filtering constraint, such that the vortex must pass through a box bounded by 20–36.5°N and 60–80°E; here we subset these further by requiring that the tracks have genesis north of 25°N (this filters out remnants of midtropospheric cyclones, which are not WDs and do not interact with the jet) and that they pass east of 70°E (this is the western edge of the Tibetan Plateau). These criteria remove approximately one third of the tracks and improve consistency with the TPV database.

#### 2.1.2. Tibetan Plateau Vortices

For TPVs, we use the database produced by Curio et al. (2018) using the objective feature-tracking algorithm TRACK (Hodges, 1994, 1995, 1999). They identified and tracked TPVs as maxima in the spectrally band-passed (T40-T100) 500 hPa relative vorticity field from ERA-Interim (1979–2015). Vortices originating within the area of the Tibetan Plateau were retained, defined by the smoothed 3,000 m altitude contour, and which persisted for at least 1 day. For this study, we only select TPVs that pass through a box with the boundaries 32–36°N and 80–87°E, which covers the region with the climatologically highest track densities. Even though the two filters described use different spectral band passing to capture events of similar wavelength, both the WD and TPV methods have been shown to produce accurate data sets for their respective targets.

### 2.2. Definition of Jet-Related Quantities

To evaluate aspects of jet position and strength or large-scale controls on the jet, we define various quantities below. All are computed using instantaneous 6-hourly ERA-Interim reanalysis data (Dee et al., 2011), from which monthly statistics can be derived.

#### 2.2.1. $p_{\text{jet}}$

To assess the mean location and probability of existence of the jet,  $p_{\text{jet}}$  is defined after Schiemann et al. (2009) as

$$p_{\text{jet}} = \begin{cases} 1 & u > 0 \text{ and } |\mathbf{u}| > 30 \text{ ms}^{-1} \\ 0 & \text{otherwise} \end{cases}. \quad (1)$$

#### 2.2.2. Baroclinicity

The metric of baroclinicity used here is the angle between local density and pressure isosurfaces, which for the small angles and fields with small horizontal gradients involved are approximated by the baroclinic term in the vorticity tendency equation. Thus,

$$B_c = \theta_{\rho\rho} \simeq k \|\nabla \rho \times \nabla p\|, \quad (2)$$

where  $\theta_{\rho\rho}$  is the local angle between the surfaces and  $k$  is some constant.

#### 2.2.3. Barotropicity

Following Kuo (1949), we use the following metric of barotropicity:

$$B_t = \begin{cases} \frac{\partial^2 u}{\partial y^2} \beta - \frac{\partial^2 u}{\partial y^2} < 0 \\ 0 & \text{otherwise} \end{cases}, \quad (3)$$

where  $u$  is the zonal component of wind,  $y$  is the meridional distance from the equator, and  $\beta$  is the meridional gradient of the Coriolis parameter.

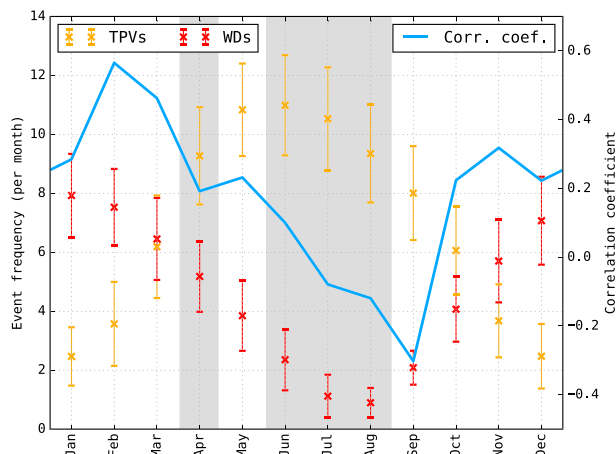


**Figure 2.** Monthly mean frequencies of WDs (red whiskers) and TPVs (yellow whiskers) with the interannual correlation between the two populations (blue line). Error bars mark one standard deviation. Where the correlation coefficient is not significant at the 10% significance level, the background has been colored gray. Monthly frequencies have been smoothed by averaging with the mean of the two neighboring months. WDs = western disturbances; TPVs = Tibetan Plateau vortices.

### 3. Results

Figure 2 shows the monthly mean frequencies for TPVs (yellow) and WDs (red), with their respective  $\pm 1\sigma$  error bars. The mean annual cycles are strongly anticorrelated (coefficient of  $-0.83$ ), while the peaks/troughs of occurrence coincide with the timing of the latitudinal extremes of the jet through the annual cycle. TPV occurrence peaks in May/June as the northern (cyclonic) half of the jet passes over the northern Tibetan Plateau, while WDs occur most often in January when the northern half of the jet typically resides over the Hindu Kush-Himalaya region. There is a varying, but significant, relationship between WD and TPV occurrence on interannual time scales (blue curve in Figure 2): the correlation coefficients vary from  $-0.30$  in September to  $0.57$  in February; during the Indian summer monsoon, when the frequencies of WDs are almost negligible, the correlation is not significant. We might surmise, therefore, that the anticorrelation in seasonal cycle indicates influence by the jet latitude, whereas the generally positive correlations in interannual frequencies indicate influence by internal variability (e.g., speed) of the jet, or some other factor.

To investigate further, we correlate the interannual frequencies with various jet properties for selected months. In Figure 3, the relationship with jet location is explored using  $p_{jet}$  (equation (1)). The mean monthly  $p_{jet}$  is regressed against three values: the total count of TPVs and WDs (colored contours, where significant at the 5% significance level), TPV counts only

(hashing, where significant at the 5% significance level, and where sign matches previous regression), and WD counts only (stippling, criteria as previous). Figure 3c is constructed slightly differently owing to the anti-correlation between TPVs and WDs in September: the *total* count is computed as the difference between the two populations rather than their sum.

In February (Figure 3a), if the jet is too far south, or north of the Tibetan Plateau, then there is reduced vortex production, largely due to failed incidence of jet on the Hindu Kush-Himalaya region and consequent reduction in WD number. In May (Figure 3b), the key south-to-north transition season of the jet as the Asian monsoon develops, a dipole structure emerges: it is more favorable to have the jet aligned with the southern edge of the Tibetan Plateau where it can affect both TPVs and WDs, rather than the northern edge where it is not typically associated with vortex generation.

This suggests that delayed northward passage of the jet through the annual cycle would yield greater numbers of WDs and TPVs than in other years. In September (Figure 3c), late southward movement of the jet is related to both an increase in TPVs and a decrease in WDs. This indicates a more subtle relationship, given the positioning of the area of positive correlation to the north of the plateau. Here the influence on vortex production cannot be direct, but may be indirect through modulation of surface heating (e.g., Kuang & Zhang, 2005) or through the support of upper-level divergence on the southern flank of the jet (e.g., Li, Zhang, Wen, & Liu, 2014).

Having analyzed the interannual relationships between WDs and TPVs and the jet position, we now explore how they are connected to internal variability of the jet. Figure 4 shows the correlation of combined WD and TPV frequencies with 200 hPa  $B_c$  (see equation (2), with significance as in Figure 3).

In February (Figure 4a), higher baroclinicity over the Arabian Sea and peninsular India, which is associated with a low-latitude jet, is detrimental to vortex production, affecting both WD and TPV generation. In contrast, there is an extended area around  $30^\circ\text{N}$  where the correlation is highly positive (for the total as well as the individual populations); the absence of this signal in Figure 3a indicates that internal jet variability is more likely than jet latitude to modulate vortex production during boreal winter. In May (Figure 4b), the anticorrelation signal largely disappears since the climatological jet position has moved north of these latitudes ( $\sim 25^\circ\text{N}$ ) by this time of year, but the area where positive baroclinicity is important remains, albeit reduced in size. In September (Figure 4c), higher TPV production and lower WD production are both associated with reduced baroclinicity to the southwest of the plateau. The latter relationship is simple, less baroclinic vorticity tendency upstream means less spin-up for instabilities in the jet. The former is less direct, a more stable jet will produce

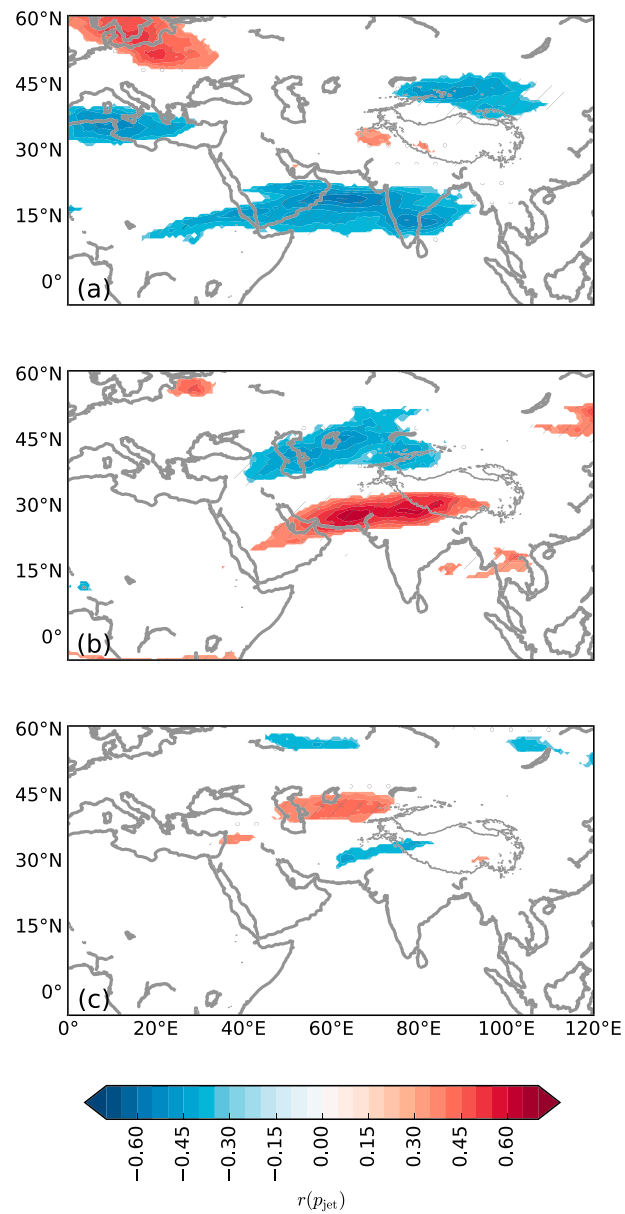


**Figure 3.** Spatial correlation coefficients between monthly mean subtropical westerly jet position (200 hPa) and monthly mean frequency of synoptic events, here defined as the sum of WD and TPV frequencies; for (a) February, (b) May, and (c) September (for which the total population is defined as TPVs minus WDs). If the sign of this matches with that of the coefficients for the individual WD and TPV populations, the area is stippled or hashed, respectively. Contours (and other markings) are only shown where the correlation coefficient is significantly different from zero at the 5% significance level. The 3,500 m orography isohypse is given in gray. WD = western disturbance; TPV = Tibetan Plateau vortex.

less large-scale cloudiness downstream (e.g., Riehl, 1948), permitting stronger sensible heating of the plateau and hence a potential increase in TPV frequency.

Some further predictors were examined: zonal wind speed,  $u$ , and barotropicity,  $B_t$  (see equation (3)). Repeating the earlier regression analyses but not shown here, correlations with  $u$  resembled those with  $p_{jet}$ ; while they are smoother and generally cover a greater area of significance, the coefficients were typically smaller. Correlations with  $B_t$  bear similarity to those with  $B_c$ , though with smaller areas of significance, pointing to the importance of both barotropic and baroclinic instabilities in the growth of WDs and TPVs.

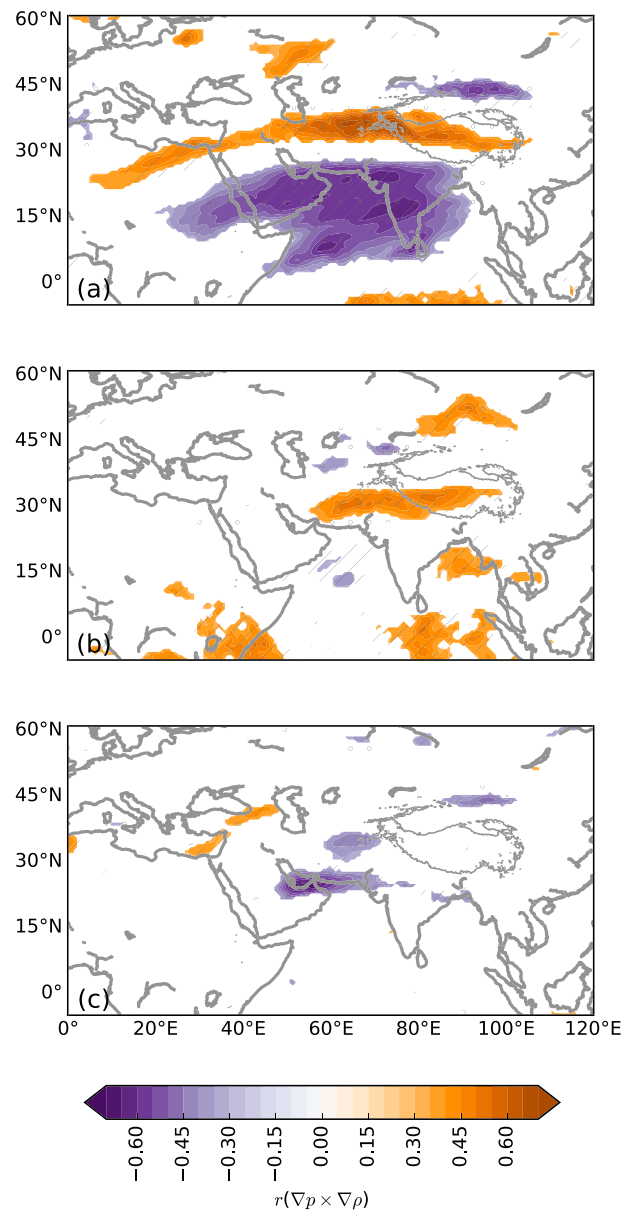


**Figure 4.** As Figure 3 but for synoptic populations regressed against upper-tropospheric (200 hPa) baroclinicity, rather than jet position.

Also considered was a modified  $u$  ( $u'$ ), where the contribution from a linear regression of WD and TPV counts onto  $p_{jet}$  was first subtracted, to mitigate against the contribution from jet position. However, correlations with  $u'$  are weak.

#### 4. Discussion and Conclusions

Bearing in mind the seasonal cycles of WDs and TPVs shown in Figure 2, the previously demonstrated relationship between WDs and the jet, and that the WDs and TPVs are dynamically similar, it is highly likely that jet position strongly influences the year-round variability of vortex production in this region.

It is also clear that during the boreal winter and spring, jet latitudinal position has an important relationship with TPV and WD interannual frequencies (Figures 3a and 3b), but these occurrence frequencies are more strongly correlated with metrics of available potential energy in the jet (e.g., baroclinicity, Figures 4a and 4b). These correlations with internal variability appear to break down during the Indian monsoon.

Figure 4a indicates a strong correlation between upper-level baroclinicity and vortex frequency in February. The most notable feature is the tongue of positive correlation reaching through north India into the Tibetan Plateau. This signal is distinct from that seen in  $p_{jet}$ , similar to but stronger than that seen in barotropicity at the same altitude, and also present to some extent in May (Figure 4b). So recalling that WDs are largely baroclinic in nature (Hunt et al., 2017) and noting the highly covariant relationship between WDs and TPVs, we deduce that TPVs are also primarily baroclinic vortices. Further, it is clear that upper-level baroclinicity plays an important role, alongside jet latitudinal position, in modulating the interannual variability of WD and TPV occurrence frequencies, as well as their sum. A marked weakening of this signal in September (Figure 4c), following general loss of significance of the TPV-WD relationship during the Indian summer monsoon, indicates that it is unlikely that variability of the jet is a significant predictor of interannual WD and TPV frequency at this time of year.

The work presented here indicates the need for a future study to compare the structures of WDs and TPVs. If they can be shown to be inseparable but for the effects of the Tibetan Plateau and different sources of moisture, then, in the context of the results presented here, it could be concluded that they are the same type of system. Furthermore, it is not necessarily clear why the sign of the interannual correlation between WDs and TPVs changes sign in September.

Regardless of their dynamical similarity, we have shown that for both TPVs and WDs, their frequencies are strongly influenced first by the location and second by the internal variability of the subtropical westerly jet. Given that there is some skill in seasonal forecasts of this jet (Li & Lin, 2015; Sonawane et al., 2015), further work could determine whether that skill can be projected onto WD and TPV frequency.

Finally, as has been shown previously (Chen et al., 1996), TPVs can interact constructively with lower-tropospheric southwest vortices to generate extreme precipitation in south China. However, it has been shown that WDs frequently propagate into south China and beyond (Hunt et al., 2017), yet no work has yet been done to quantify the interaction (should there be one) between WDs and SWVs. If TPVs and WDs are indeed dynamically and thermodynamically similar (as has been suggested by previous work; e.g., Feng et al., 2017; Hunt et al., 2017; Wang, 1987), and carry a correlated risk (as has been suggested here), then such interactions could potentially lead to very strong impacts, and therefore require further study.

#### Acknowledgments

This study was partially supported by the JPI-Climate and Belmont Forum Climate Predictability and Inter-Regional Linkages Collaborative Research Action via NERC Grant NE/P006795/1 (authors KMRH and AGT) and by the UK-China Research and Innovation Partnership Fund through the Met Office Climate Science for Service Partnership (CSSP) China as part of the Newton Fund Grant agreement P100195 between the Met Office and the National Centre for Atmospheric Science at the University of Reading for the MESETA project (authors JC, RS, and AGT). No new data were used in producing this manuscript.

#### References

- Chen, B.-M., Qian, Z., & Zhang, L.-S. (1996). Numerical simulation of the formation and development of vortices over the Qinghai-Xizang Plateau in summer. *Scientia Atmosferica Sinica*, 20, 491–502.
- Curio, J., Chen, Y., Schiemann, R., Turner, A. G., Wong, K. C., Hodges, K. I., & Li, Y. (2018). Comparison of a manual and an automated tracking method for Tibetan Plateau vortices. *Advances in Atmospheric Sciences*, 35(8), 965–980. <https://doi.org/10.1007/s00376-018-7278-4>
- Dee, D. P., Uppala, S. M., Simmons, A. J., Berrisford, P., Poli, P., Kobayashi, S., et al. (2011). The ERA-Interim reanalysis: Configuration and performance of the data assimilation system. *Quarterly Journal of the Royal Meteorological Society*, 137(656), 553–597. <https://doi.org/10.1002/qj.828>
- Dell'Osso, L., & Chen, S.-J. (1986). Numerical experiments on the genesis of vortices over the Qinghai-Tibet plateau. *Tellus A*, 38(3), 236–250.
- Dimri, A. P. (2004). Impact of horizontal model resolution and orography on the simulation of a western disturbance and its associated precipitation. *Meteorological Applications*, 11(2), 115–127.
- Feng, X.-Y., Liu, C.-H., Fan, G.-Z., Liu, X.-D., & Feng, C.-Y. (2016). Climatology and structures of southwest vortices in the NCEP climate forecast system reanalysis. *Journal of Climate*, 29(21), 7675–7701.
- Feng, X.-Y., Liu, C.-H., Fan, G.-Z., & Zhang, J. (2017). Analysis of the structure of different Tibetan Plateau vortex types. *Journal of Meteorological Research*, 31(3), 514–529.
- Feng, X.-Y., Liu, C.-H., Rasmussen, R., & Fan, G.-Z. (2014). A 10-yr climatology of Tibetan Plateau vortices with NCEP climate forecast system reanalysis. *Journal of Applied Meteorology and Climatology*, 53(1), 34–46.
- Hodges, K. I. (1994). A general-method for tracking analysis and its application to meteorological data. *Monthly Weather Review*, 122(11), 2573–2586.
- Hodges, K. I. (1995). Feature tracking on the unit sphere. *Monthly Weather Review*, 123(12), 3458–3465.
- Hodges, K. I. (1999). Adaptive constraints for feature tracking. *Monthly Weather Review*, 127(6), 1362–1373.
- Hunt, K. M. R., Turner, A. G., & Shaffrey, L. C. (2017). The evolution, seasonality, and impacts of Western disturbances. *Quarterly Journal of the Royal Meteorological Society*, 144(710), 278–290. <https://doi.org/10.1002/qj.3200>
- Hunt, K. M. R., Turner, A. G., & Shaffrey, L. C. (2018). Extreme daily rainfall in Pakistan and North India: Scale-interactions, mechanisms, and precursors. *Monthly Weather Review*. <https://doi.org/10.1175/MWR-D-17-0258.1> in press.
- Kuang, X.-Y., & Zhang, Y.-C. (2005). Seasonal variation of the East Asian subtropical westerly jet and its association with the heating field over East Asia. *Advances in Atmospheric Sciences*, 22(6), 831–840.
- Kuo, H.-L. (1949). Dynamic instability of two-dimensional nondivergent flow in a barotropic atmosphere. *Journal of Meteorology*, 6(2), 105–122.
- Li, C.-F., & Lin, Z.-D. (2015). Predictability of the summer East Asian upper-tropospheric westerly jet in ENSEMBLES multi-model forecasts. *Advances in Atmospheric Sciences*, 32(12), 1669–1682.
- Li, G.-P., & Liu, H.-W. (2006). A dynamical study of the role of surface heating on the Tibetan Plateau vortices. *Journal of Tropical Meteorology*, 22(6), 632–637.

- Li, L., Zhang, R.-H., & Wen, M. (2011). Diagnostic analysis of the evolution mechanism for a vortex over the Tibetan Plateau in June 2008. *Advances in Atmospheric Sciences*, 28(4), 797–808.
- Li, L., Zhang, R.-H., & Wen, M. (2014). Diurnal variation in the occurrence frequency of the Tibetan Plateau vortices. *Meteorology and Atmospheric Physics*, 125(3–4), 135–144.
- Li, L., Zhang, R.-H., & Wen, M. (2017). Genesis of southwest vortices and its relation to Tibetan Plateau vortices. *Quarterly Journal of the Royal Meteorological Society*, 143(707), 2556–2566.
- Li, L., Zhang, R.-H., Wen, M., & Liu, L.-K. (2014). Effect of the atmospheric heat source on the development and eastward movement of the Tibetan Plateau vortices. *Tellus A*, 66(1), 24451.
- Li, G.-P., Zhao, B.-J., & Yang, J.-Q. (2002). A dynamical study of the role of surface sensible heating in the structure and intensification of the Tibetan Plateau vortices. *Chinese Journal of Atmospheric Sciences*, 26(4), 519–525.
- Mull, S., & Desai, B. N. (1947). The origin and structure of the winter depression of Northwest India (Technical note, No. 25). India: India Meteorological Department.
- Pisharoty, P. R., & Desai, B. N. (1956). Western disturbances and Indian weather. *Indian Journal of Meteorology & Geophysics*, 7, 333–338.
- Raju, P. V. S., Bhatla, R., & Mohanty, U. C. (2011). A study on certain aspects of kinetic energy associated with western disturbances over Northwest India. *Atmós*, 24(4), 375–384.
- Ramanathan, V., & Saha, K. R. (1972). Application of a primitive equation barotropic model to predict movement of "western disturbances". *Journal of Applied Meteorology*, 11(2), 268–272.
- Riehl, G. (1948). Jet stream in upper troposphere and cyclone formation. *Transactions, American Geophysical Union*, 29(2), 175–186.
- Schiemann, R., Lüthi, D., & Schär, C. (2009). Seasonality and interannual variability of the westerly jet in the Tibetan Plateau region. *Journal of Climate*, 22(11), 2940–2957.
- Sonawane, K., Sreejith, O. P., Pattanaik, D. R., Benke, M., Patil, N., & Pai, D. S. (2015). Simulation of Indian summer monsoon using the Japan meteorological agency's seasonal ensemble prediction system. *Journal of Earth System Science*, 124(2), 321–333.
- Tao, S.-Y., & Ding, Y.-H. (1981). Observational evidence of the influence of the Qinghai-Xizang (Tibet) Plateau on the occurrence of heavy rain and severe convective storms in China. *Bulletin of the American Meteorological Society*, 62(1), 23–30.
- Wang, B. (1987). The development mechanism for Tibetan Plateau warm vortices. *Journal of the Atmospheric Sciences*, 44(20), 2978–2994.
- Zheng, Y.-J., Wu, G.-X., & Liu, Y.-M. (2013). Dynamical and thermal problems in vortex development and movement. Part I: A PV-Q view. *Acta Meteorologica Sinica*, 27(1), 1–14.